

Table 1. Effective media for somatic embryogenesis of teak

| Explant | Type of somatic embryogenesis | Medium | Remarks |
|------------------------|-------------------------------|-----------------------------------------------------|---------------------------------------------------|
| Callus of apical bud | Indirect | Full strength MS + BAP (0.1 mg/l) + NAA (0.01 mg/l) | Semisolid medium in test tubes |
| Callus of axillary bud | Indirect | ½ MS + BAP (0.5 mg/l) + NAA (0.1 mg/l) | Liquid medium in test tubes and Erlenmeyer flasks |
| Axillary bud | Direct | ½ MS + BAP (1.0 mg/l) + 2iP (1.5 mg/l) | Liquid medium in test tubes having paper rafts |

from apical buds needed full strength MS medium. Requirement of full strength MS medium was also found in case of apple⁷.

Efforts are on to further differentiate these somatic embryos into plantlets.

1. Gupta, P. K., Nadgir, A. L., Mascarenhas, A. F. and Jagannathan, V., *Plant Sci. Lett.*, 1980, **17**, 259-268.
2. Devi, S. Y., Mukherjee, B. B. and Gupta, S., *Indian J. Exp. Biol.*, 1994, **32**, 668-671.
3. Harini, I., Nair, A. C. and Subramani, J., 8th International Congress of Plant Tissue and Cell Culture, Firenze, 1994, Abstracts, p. 6.

4. Murashige, T. and Skoog, F., *Physiol. Plant.*, 1962, **15**, 473-479.
5. Litz, R. E., Knight, R. J. and Gazit, S., *Plant Cell Rep.*, 1982, **1**, 264-266.
6. Raemakers, C. J. J. M., Schavemaker, C. M., Jacobsen, E. and Visser, R. G. F., *Plant Cell Rep.*, 1993, **12**, 226-229.
7. Milewska, P. E. and Kubicki, B., *Acta Hort.*, 1977, **78**, 271-276.

ACKNOWLEDGEMENTS. We thank C. C. Shroff Research Institute and Excel Industries Ltd., Mumbai for financial support.

Received 6 February 1996; revised accepted 16 October 1996

Onset of an arid climate at 3.5 ka in the tropics: Evidence from monsoon upwelling record

Pothuri Divakar Naidu

National Institute of Oceanography, Dona Paula, Goa 403 004, India

Studies on the variability of Southwest (SW) monsoon strength using the monsoon upwelling indices (fluxes of total planktonic foraminifera and *Globigerina bulloides*) from the western Arabian Sea reveal that the weakening phase of the SW monsoon started from 5 ka (ka = 1000 years). The intensity of monsoon returned to glacial strength at 3.5 ka, coinciding with the onset of arid climate elsewhere in the tropics. The onset of the weak phase of the monsoon and arid climate at 3.5 ka appears to be a primary reason for the decline of Indus Valley Civilization, major change in vegetation along the Western Ghats and decrease of river discharge from all major rivers during that period.

DURING the Northern Hemisphere summer, strong south-westerly monsoon winds blow across the Arabian Sea, causing offshore Ekman transport and intense seasonal upwelling along the Oman and Somalia margins and the Southwest coast of India¹⁻⁴. The upwelling

process brings cold, nutrient-rich waters from a few hundred meters depth to the surface and increases biological productivity in the euphotic zone. During the winter, the Northeast monsoon winds invoke onshore Ekman transport of surface waters, which suppresses upwelling and lowers the productivity along the continental margin of the western Indian Ocean. Thus the south-westerly and north-easterly winds produce a striking seasonal contrast in primary productivity⁵ and biogenic and lithogenic fluxes⁶ in the Arabian Sea. Distinctive plankton faunas and floras thrive in the upwelling waters and are eventually incorporated into the sediments on the sea floor, producing a geological record of upwelling. The sedimentary record in the Arabian Sea is thus linked to the strength of the SW monsoon winds and associated rainfall in southeast Asia. The biogeochemical studies on these sediments therefore provide valuable information on the variability of monsoon upwelling and rainfall in southeast Asian countries over geological time scales. Recently, we have documented the general variability of the SW monsoon for the last 19 ka and its sub-Milankovitch cyclicality^{7,8}. The primary tasks leading to this communication were (i) to find out when the weakening phase of SW monsoon was set in within the late Holocene, and (ii) whether this time coincided with rapid climate shifts elsewhere in the tropics.

The upper 7.4 m of the Ocean Drilling Program (ODP) Hole 723A (Figure 1) was sampled at 10 cm interval, which gives an approximate time resolution of 250 years. Radio carbon dates obtained on Accelerated Mass Spectrometry (AMS) were used to establish the chronology (Table 1). High resolution upwelling indices data in conjunction with precise AMS radiocarbon chronology, permit a detailed interpretation of SW monsoon variability and climate change from the tropical Arabian Sea. The details about the AMS dates and upwelling indices are discussed elsewhere⁷.

Several planktonic foraminiferal indices of upwelling were identified in the Arabian Sea⁹⁻¹¹. Fluxes of total planktonic foraminifera and *Globigerina bulloides* were used to measure the upwelling intensity in the western Arabian Sea and in turn the SW monsoon strength in south Asia.

It has been well established that the SW monsoon was weaker during glacial periods and stronger during interglacials¹². Intensification of the SW monsoon started at 12 ka, i.e. after a weak phase during the last glacial period¹³. Within the Holocene, greater values of upwelling indices have been noted between 10 and 6 ka, reflecting

a strong SW monsoon (Figure 2). The values of upwelling indices decrease abruptly at 5 ka, indicating a weakening of the SW monsoon. The lowest upwelling indices in the Holocene occurs between 3.5 and 1.2 ka (Figure 2), suggesting that upwelling and the SW monsoon intensity decreased during this period. At 3.5 ka the upwelling indices exhibit the same values as that at 12 ka, when the monsoon started its intensification after the last glacial period, and from 3.5 ka the upwelling indices decline further. Other evidences such as water levels in Ethiopian lakes¹⁴, palaeohydrological data from western Tibet¹⁵, benthic foraminifera record from eastern Arabian Sea¹⁶, pollen records from Northwest India¹⁷ and $\delta^{13}\text{C}$ values of peat deposits¹⁸ also suggest a weaker SW monsoon during this time. A similar pattern of dry conditions during the late Holocene is also reported from Africa and the regions around Caribbean.

Independent evidences such as pollen studies from the eastern Arabian Sea¹⁹, and down core variations of calcium carbonate in the western Arabian Sea²⁰ and $\delta^{18}\text{O}$ data from Tibet lakes¹⁵ also document the arid climate during this time. This observation is further corroborated by an abrupt change in solar radiation, precipitation,

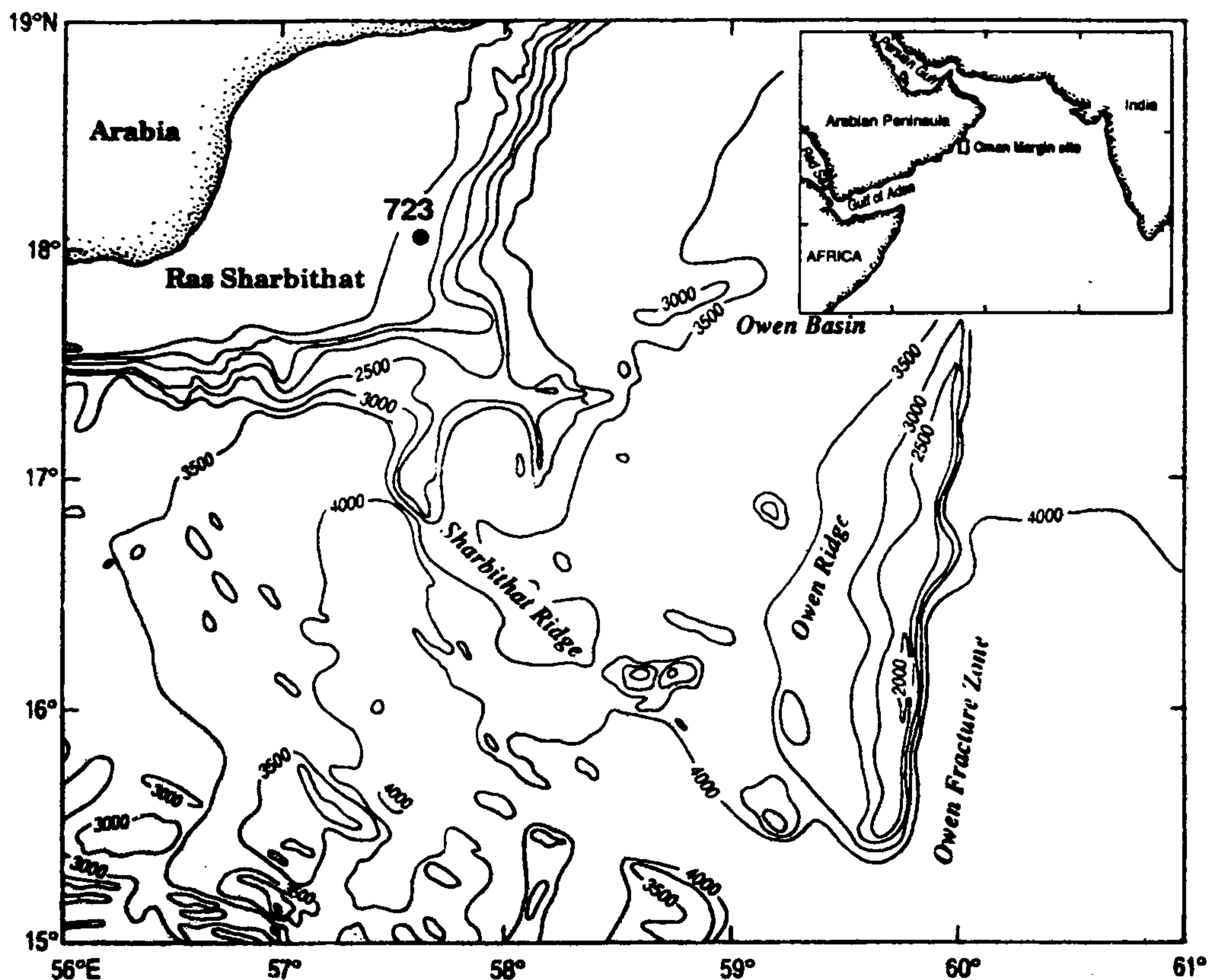


Figure 1. Location of ODP Site 723A, physiography and bathymetry (in metres) of the western Arabian Sea.

Table 1. Radiocarbon ages for ODP Site 723A determined using Accelerator Mass Spectrometer at The Svedberg Laboratory, Uppsala University, Sweden. After Naidu and Malmgren⁵.

| Core | Section | Sampling depth (cm) | ¹⁴ C ages (years BP) | Error years |
|------|---------|---------------------|---------------------------------|-------------|
| 1H | 1 | 3 | 950 | ± 55 |
| 1H | 2 | 160 | 5,865 | ± 65 |
| 1H | 3 | 290 | 9,100 | ± 90 |
| 1H | 4 | 520 | 15,920 | ± 125 |
| 1H | 5 | 740 | 19,130 | ± 275 |

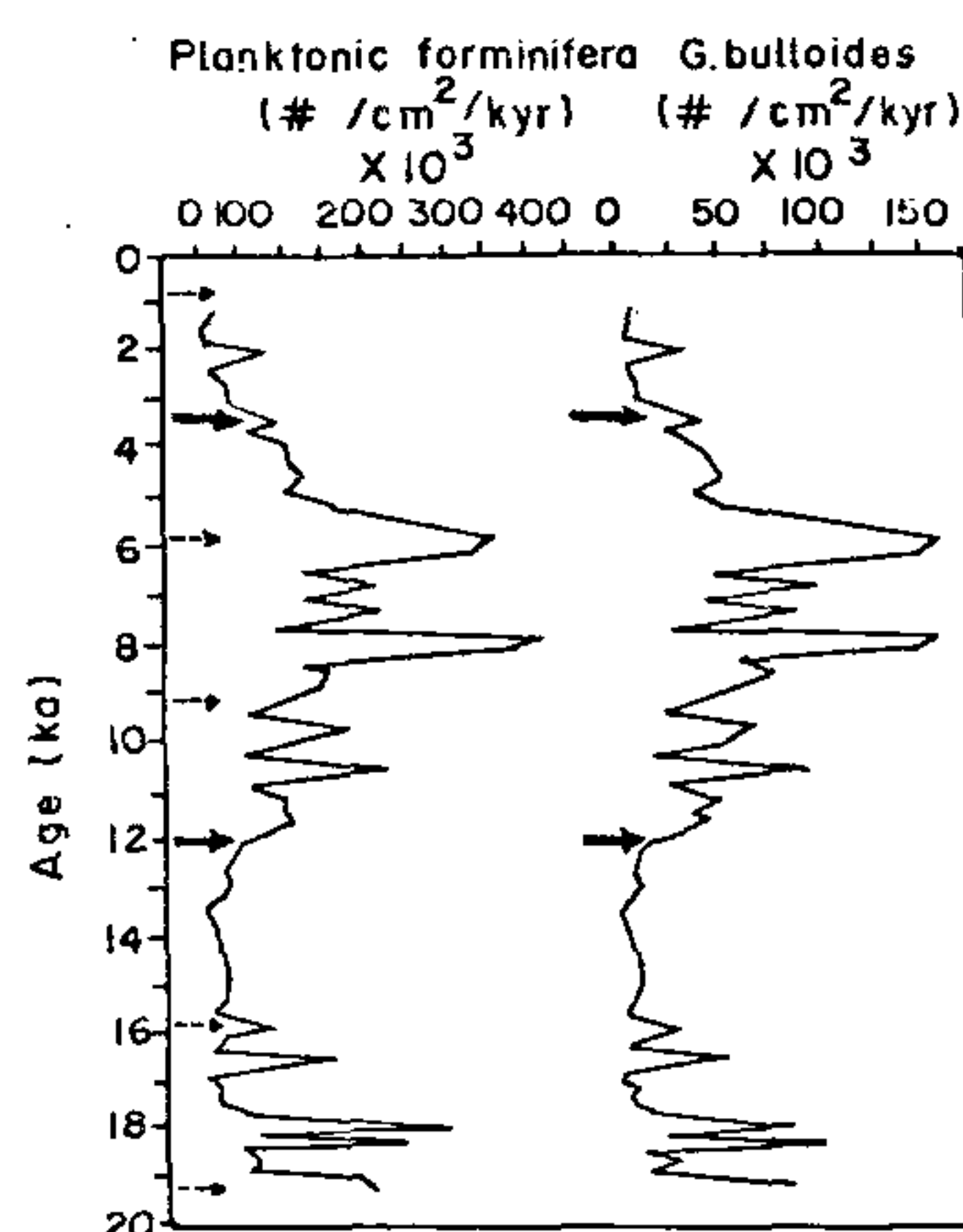


Figure 2. Fluctuations in fluxes of total planktonic foraminiferal shells (>150 μm fraction) and *Globigerina bulloides*. Ages were based on five AMS ¹⁴C dates at levels marked by dotted arrows. Thick arrows mark the start of monsoon intensification after glaciation (at 12 ka) and the weakening phase of monsoon during late Holocene (at 3.5 ka).

temperature and southwesterly winds at about 3.5 ka in the Arabian Sea²¹. The recent (2–4 ka) aeolian activity in the Thar Desert²² also corresponds with the onset of arid climate at 3.5 ka. Dry episodes including the current drought in the Sahel have been correlated with warming of the surface ocean in the southern hemisphere and the north Indian Ocean, and cooling of the North Atlantic and the North Pacific. The declining strength of the SW monsoon since 3.5 ka can therefore be interpreted as a result of the onset of arid climate in general throughout the tropics and in particular in the Asian tropics.

The onset of arid climate and decline of the SW monsoon at 3.5 ka was resulted in a change in the vegetation along the Western Ghats¹⁹. *Casuarina*, *Callitris* shrubs and ferns declined during this period in South Australia²³. The Godavari, Bhima and Krishna rivers originate in the elevated region of the Western Ghats, and their discharge depends on the precipitation driven by the SW monsoon winds. These rivers discharge and lake levels in India, Africa, Australia and China also

dropped during that time. It was previously pointed out that neotectonism was responsible for the drying of the Sarasvati River²⁴. This event could, however, also be attributed to drastic climatic changes at 3.5 ka. It is well established that the down fall of Chalcolithic Cultures (about one million BC) is ascribed to severe droughts in western and central India, similarly the decline of the Indus Valley Civilization around 3.5 ka could be due to the onset of arid climate at 3.5 ka.

An obvious, but provocative question is whether the onset of arid climate at 3.5 ka is traceable in other tropical regions of the world. Evidences such as ¹⁸O/¹⁶O ratios in ostracod shells from Caribbean lakes²⁵ and pollen analysis from south Australia lake²³ have also documented the onset of an arid phase at 3.5 ka. Thus the onset of arid climate at 3.5 ka appears to be a global event, prevailing throughout the late Holocene.

Coherent occurrence of an arid climate at 3.5 ka in the northern hemisphere (present study) and southern hemisphere²⁵, and synchronous dropping and raising of water levels in Australia and China²⁶ indicate that late Holocene climate in the tropics of both hemispheres were in phase.

Two theories, viz. Milankovitch orbital theory²⁷ and deep water formation changes²⁸ have been put forward to explain the causes of glaciation and deglaciation in the Quaternary period. The Milankovitch orbital theory explains the general envelope of past glacial climatic changes, but does not explain either the timing or the amplitude of short-term changes noticed in the present study and in ice core records²⁸. On the other hand, deep water formation changes provide a more satisfactory hypothesis for explaining the ultra fast and abrupt climatic shifts in the ice cores²⁹, and marine sediment records³⁰.

It has been pointed out that thermohaline circulation changes have an influence on the rainfall in the tropics³¹. Deep water formations in the North Atlantic have a profound influence in causing the abrupt climatic shifts at high latitudes³² and probably in low latitudes too. Therefore, I suggest the missing link between the thermohaline circulation and/or deep water formations at high latitudes and monsoon intensity may be initiated to understand the onset of arid climate in the tropics and decrease of monsoon strength.

To conclude, high resolution data on upwelling indices, in conjunction with precise AMS radiocarbon chronology, permit a detailed interpretation of SW monsoon variability and climate change in the tropical Arabian Sea. The decreasing upwelling indices since 5 ka reflect a recent weakening of the SW monsoon, with the weakest phase taking place at 3.5 ka, which coincided with the onset of arid climate in other parts of tropics. The onset of arid climate during that time appears to be the main cause of declining vegetation and river discharge in the Indian subcontinent during that period. The drastic cli-

mate shift at 3.5 ka might be one of the reasons for the decline of Indus Valley Civilization.

1. Wyrki, K., *The Biology of the Indian Ocean*, Springer, New York, 1973, pp. 18-36.
2. Schott, W., 'Meteor' 1925-1927, *Wiss. Ergeb*, 1935, 3, 43-134.
3. Shallow, J. C., *Deep-Sea Res.*, 1984, 31, 639-650.
4. Bauer, S., Hitchcock, G. L. and Olson, D. B., *Deep-Sea Res.*, 1991, 38, 531-553.
5. Kobanova, Y. G., *Oceanology*, 1968, 8, 214.
6. Nair, R. R., Ittekkot, V., Manganini, S. J., Ramaswamy, V., Haake, B., Degens, E. T., Desai, B. and Honjo, S., *Nature*, 1989, 338, 749-751.
7. Naidu, P. D. and Malmgren, B. A., *Paleoceanography*, 1995, 10, 117-122.
8. Naidu, P. D. and Malmgren, B. A., *Geophys. Res. Lett.*, 1995, 22, 2361-2364.
9. Prell, W. L., *Milankovitch and Climate*, Part I, D. Reidel, Hingham, 1984, pp. 349-366.
10. Naidu, P. D., *Oceanologica Acta*, 1990, 13, 327-333.
11. Naidu, P. D., Babu, C. P. and Rao, Ch. M., *Deep-Sea Res.*, 1992, 39, 715-723.
12. Anderson, D. M. and Prell, W. L., *Paleoceanography*, 1993, 8, 193-208.
13. Naidu, P. D. and Malmgren, B. A., *Paleoceanography*, 1996, 11, 129-140.
14. Gillespie, R., Street Perrott, F. A. and Switzen, R., *Nature*, 1983, 306, 680-683.
15. Gasse, F. and van Campo, E., *Earth Planet. Sci. Lett.*, 1994, 126, 435-456.
16. Nigam, R., *Curr. Sci.*, 1993, 64, 935-937.
17. Singh, G., Joshi, R. D., Chopra, S. K. and Singh, A. B., *Philos. Trans. R. Soc. London Series*, 1974, 267, 467-501.
18. Sukumar, R., Ramesh, R., Pant, R. K. and Rajagopalan, G., *Nature*, 1983, 364, 703-706.
19. Caratini, C., Bentaleb, I., Fontugne, M., Morzadec-Kerfourn, M. T., Pascal, J. P. and Tissot, C., *Palaeogeogr. Palaeoclimatol. Palaeoecol.*, 1994, 109, 371-384.
20. Sirocko, F., Sarnthein, M., Erlenkeuser, H., Lange, H., Arnold, M., Duplessy, J. C., *Nature*, 1993, 364, 322-324.
21. Zahn, R., *Nature*, 1994, 372, 621-622.
22. Dhir, R. P., Rajaguru, S. N. and Singhvi, A. K., *J. Geol. Soc. India*, 1994, 43, 435-447.
23. Singh, G. and Luly, J., *Palaeogeogr. Palaeoclimatol. Palaeoecol.*, 1991, 84, 75-86.
24. Pal, Y., Sahai, B., Sood, R. K. and Agrawal, D. P., *Proc. Indian Acad. Sci. (Earth Planet. Sci.)*, 1980, 89, 317-331.
25. Hodell, D. A. et al., *Nature*, 1991, 352, 790-793.
26. An, Z., Kukla, G. J. Porter, S. G. and Xiao, J., *Quat. Res.*, 1991, 36, 29-36.
27. Imbrie, J. et al., *Paleoceanography*, 1992, 7, 701-738.
28. Broecker, W. S. and Denton, G. H., *Geochim. Cosmochim. Acta*, 1990, 53, 2465-2501.
29. Dansgaard, W. et al., *Nature*, 1993, 364, 218-220.
30. Bond, G. et al., *Nature*, 1993, 365, 143-145.
31. Street, F. A. and Perrott, R. A., *Nature*, 1990, 343, 607-612.
32. Broecker, W. S. and Denton, G. H., *Sci. Am.*, 1990, pp. 43-50.

ACKNOWLEDGEMENTS. I would like to thank E. Desa, Director and R. R. Nair, Deputy Director for their suggestions and support. Ocean Drilling Programme (ODP) supplied the samples for this study. The study was financially supported by Swedish Natural Science Research Council, Sweden.

Received 27 May 1996; revised accepted 30 September 1996

Precambrian-Cambrian boundary microbiota from the Chert Phosphorite Member of Tal Formation in the Korgai Syncline, Lesser Himalaya, India

Meera Tiwari

Wadia Institute of Himalayan Geology, Dehradun 248 001, India

Abundant and well preserved organic walled microfossils are recorded from the Chert-Phosphorite Member of the Tal Formation, in the Korgai Syncline, Lesser Himalaya. Two principal categories of microfossils including spheromorphic acritarch and small acanthomorphic acritarchs are present in the assemblage. Interesting among these two categories are *Leiospheridea* sp., *Micrhystridium regulare*, *M. sp. A*, *M. sp. B*, *M. sp. C*, *M. sp. D* and *Verhachium* sp. The appearance of large *Micrhystridium* population together with small shelly fauna has been used as a criterion to demarcate the Precambrian-Cambrian boundary in China¹ where these microfossils have been discovered from the black chert in the phosphatic rocks of the lowest Kuanchuanpu Member in Ningqiang of southern Shaanxi.

THE Korgai syncline is one of the five major synclines of the Krol belt where the Blaini-Krol-Tal sequence is well exposed. It is located 15 km southeast of Nigalidhar syncline and comprises an area of about 23.50 sq km. Prior to this communication no microbiota was reported from this syncline. The material for this study was collected from a trench located in the NE of Sataun (Figure 1) approximately 4 km from Bargaun on the mule track from Bargaun to Banana village (30° 35' 16" : 77° 40' 44"). Here, the Lower Tal Formation

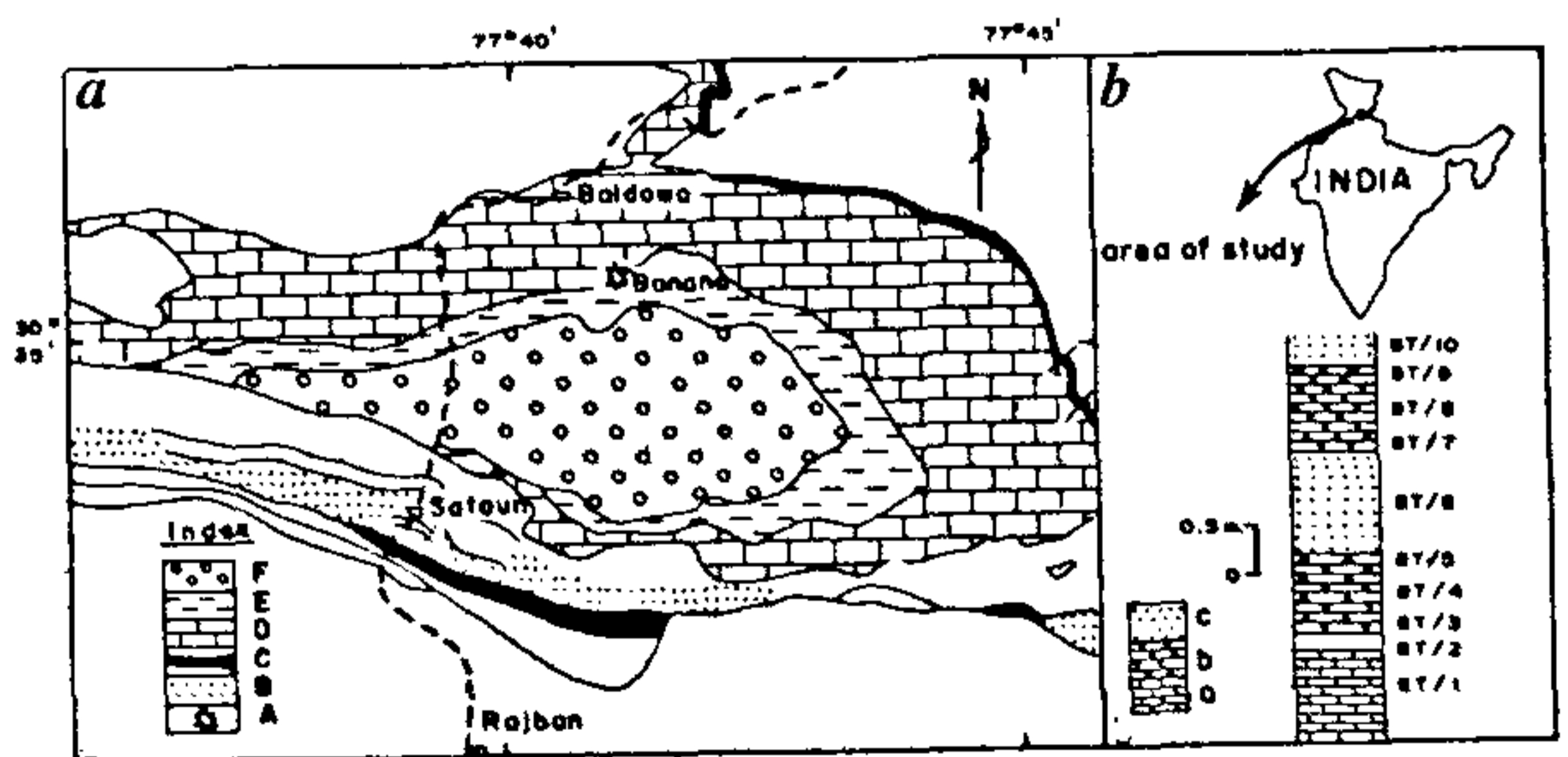


Figure 1a, b. a, Geological map of the area (after Auden, 1934) showing the fossil locality. A = Fossil locality, B = Chandpur and Nagthat formations, C = Blaini Formation, D = Krol Formation, E = Lower Tal Formation, F = Upper Tal Formation; b, Litholog showing sample interval. a = dolomitic limestone, b = cherty phosphorite, c = sandy unit.